

CondNet: Conditional Classifier for Scene Segmentation

Changqian Yu, Yuanjie Shao, Changxin Gao, Nong Sang

Abstract—The fully convolutional network (FCN) has achieved tremendous success in dense visual recognition tasks, such as scene segmentation. The last layer of FCN is typically a global classifier (1×1 convolution) to recognize each pixel to a semantic label. We empirically show that this global classifier, ignoring the intra-class distinction, may lead to sub-optimal results.

In this work, we present a conditional classifier to replace the traditional global classifier, where the kernels of the classifier are generated dynamically conditioned on the input. The main advantages of the new classifier consist of: (i) it attends on the intra-class distinction, leading to stronger dense recognition capability; (ii) the conditional classifier is simple and flexible to be integrated into almost arbitrary FCN architectures to improve the prediction. Extensive experiments demonstrate that the proposed classifier performs favourably against the traditional classifier on the FCN architecture. The framework equipped with the conditional classifier (called CondNet) achieves new state-of-the-art performances on two datasets. The code and models are available at <https://git.io/CondNet>.

Index Terms—Conditional classifier, dynamic convolutions, semantic segmentation

I. INTRODUCTION

SCENE segmentation [1]–[5] is a fundamental and challenging task in visual recognition, aiming to recognize each pixel into a semantic category, providing comprehensive scene understanding. It has extensive downstream applications, e.g., autonomous driving [6]–[9], human-machine interaction [10], and augmented reality.

In recent years, with the development of deep neural networks [11]–[14], the fully convolutional network (FCN) [15] has achieved tremendous success and been the dominant solution in the scene segmentation task. In the original FCNs, the whole architecture composes of a *feature extractor* and a *classifier* (the last layer for prediction).

Feature extractors have been widely studied for embedding powerful feature representation. Various designs have been proposed to extract effective discriminative features: (i) larger receptive field, e.g., dilation/deformable convolutions [16]–[18], (ii) multi-scale representation via pyramid methods,

Manuscript received January 18, 2021; revised March 10, 2021; accepted March 13, 2021. Date of publication April 1, 2021; date of current version April 28, 2021. This work is supported by the National Natural Science Foundation of China under Grants 61433007, 61876210 and 61901184. The associate editor coordinating the review of this manuscript and approving it for publication was Prof. Yue Deng. (*Corresponding author: N. Sang*)

The authors are with the Key Laboratory of Image Processing and Intelligent Control, School of Artificial Intelligence and Automation, Huazhong University of Science and Technology, Wuhan 430074, China (e-mail: changqian_yu@hust.edu.cn; shaoyuanjie@hust.edu.cn; cgao@hust.edu.cn; nsang@hust.edu.cn).

Digital Object Identifier 10.1109/LSP.2021.3070472

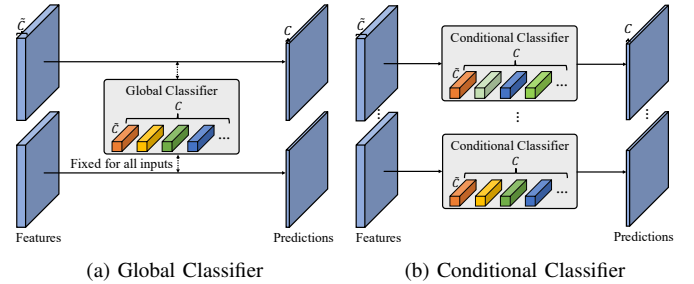


Fig. 1. Illustration of global classifier and conditional classifier. Global classifier stays fixed for all inputs. Conditional classifier generates diverse kernels for different samples conditioned on the inputs.

e.g., PPM [19], ASPP [20] and MDCCNet [4], (iii) adaptive aggregation via attention mechanism, e.g., self-attention [21]–[23] and channel attention mechanism [9], [24]–[27].

In contrast, the classifier has been studied in relatively few works. The traditional classifier performs the kernel correlation on each position of the feature map to obtain the desired pixel-wise prediction. In the training phase, the kernel is learned thorough the whole training samples. In the evaluation phase, the learned kernels stay fixed and are applied to the feature maps to predict the semantic maps. We call this type of classifier as the global classifier, which attempts to seek a **global class center** to recognize all the variation of different samples, as shown in Figure 1 (a).

The drawback of the global classifier is its limited capability to handle the intra-class distinction. In some complex scene, the diverse samples of the same semantic category may have very different appearances (which we call intra-class distinction/variation). It is common that the traditional classifier is easy to mis-recognize these pixels of the same category but different appearances into different categories since it is global for the majority of pixels of one category.

In this work, we present a conditional classifier for pixel-wise recognition, replacing the global classifier used extensively in previous works. The main idea behind our work is to generate the sample-specific kernels with parameters adapted to the particular patterns within an input sample, which can handle the intra-class distinction, as shown in Figure 1 (b).

Our conditional classifier consists of two parts: the *class-feature aggregation module* and the *kernel generation module*. The class-feature aggregation module tends to aggregate the features of each semantic category via weighted average. It is expected that the weighted average manner can capture the distinction of the same category within one sample as the **sample-specific class center** (instead of the global class

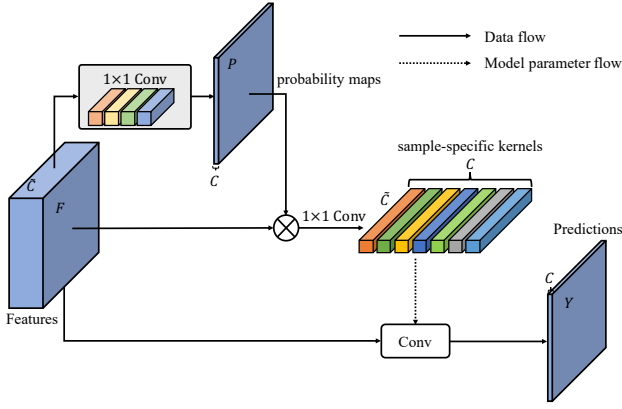


Fig. 2. **Structure of the proposed conditional classifier.** The conditional classifier aggregates the features of each semantic category as the sample-specific class centers guided by the coarse probability maps. Then, the class centers are transformed to generate the sample-specific kernels to recognize the features to the final predictions. The probability maps are generated by a 1×1 convolution.

center). The kernel generation module dynamically generates the sample-specific kernels conditioned on the sample-specific class center. The generated sample-specific kernels are applied to the input sample to predict the semantic masks.

There are several merits of the proposed conditional classifier: (i) The conditional classifier attends on the sample-specific distinction of each category to learn a more discriminative classifier. (ii) The conditional classifier can be seamlessly incorporated into almost arbitrary FCN architectures, replacing the global classifier (1×1 convolution).

Extensive evaluations on the scene segmentation task demonstrate that the conditional classifier performs favourably against the traditional classifier. The framework equipped with the conditional classifier (called **CondNet**) achieves new state-of-the-art performances on two challenging datasets.

II. PROPOSED METHOD

In this section, we first revisit the global classifier used extensively in previous works. Next, we formulate the proposed conditional classifier. Finally, we describe the overall architecture with our proposed conditional classifier and the corresponding loss functions.

A. Revisiting Global Classifier

A typical global classifier is a 1×1 convolution used as the last layer of the segmentation architecture, as shown in Figure 1 (a). Consider an input feature $F \in \mathcal{R}^{\tilde{C} \times H \times W}$ (the final output of the feature extractor), and the desired prediction $Y \in \mathcal{R}^{C \times H \times W}$, where H , W , \tilde{C} , C denote the height, width, channel dimensions, and the number of semantic categories, respectively.

The global classifier performs a matrix-vector multiplication on each position of F :

$$Y = \mathcal{H}(F, \mathbf{W}), \quad (1)$$

where \mathcal{H} is the global classifier (1×1 convolution) with the kernels $\mathbf{W} \in \mathcal{R}^{C \times \tilde{C}}$, Y is the prediction maps, and \otimes indicates

the convolutional operation. For each semantic category, the classifier has a kernel $w^s \in \mathcal{R}^{1 \times \tilde{C}}$, where $s \in \{1, 2, \dots, C\}$. After training, the kernel stays fixed and is applied to recognize all different samples (that is why we call it global classifier). Therefore, the learned kernel is required to capture all the variation between different samples of the same category to output the correct prediction. However, the different samples of the same category may have far different appearances, especially in some complex scene. We argue that the global classifier is hard to capture all variation, thus leading to sub-optimal results.

In fact, for an input image, the pixels of the same category have more similar patterns due to belonging to the same scene. In other words, the pixels of the same category in the same scene have a **sample-specific class center**, which, intuitively, is easier to recognize these pixels than the global class center. This motivates us to propose the conditional classifier, which generates the sample-specific kernels conditioned on the sample-specific class centers.

B. Conditional Classifier

The overall structure of the conditional classifier is shown in Figure 2. It mainly consists of two parts: *class-feature aggregation module* and *kernel generation module*.

a) *Class-feature aggregation*: The goal of the class-feature aggregation module is to embed the sample-specific class center. For one input sample, it requires to aggregate all the features of the same category as the class center embedding. The embedding $E^s \in \mathcal{R}^{\tilde{C}}$ is defined as the weighted average of the features belonging to the category s , as formulated as follows:

$$E^s = \frac{\sum_{j=0}^N p_j^s F_j}{N}, \quad (2)$$

where $N = H \times W$, $p^s \in \mathcal{R}^{H \times W}$ denotes the probability map belonging to category s . Here, we use the coarse prediction masks of the segmentation network as the probability maps $P \in \mathcal{R}^{C \times H \times W}$, which are generated by a 1×1 convolution.

The sample-specific class center embeddings capture the variation of different pixels within one input sample. It is easier to handle the particular patterns of one certain sample than the global class center.

b) *Kernel generation*: We use the projection \mathcal{H}_θ with kernels \mathbf{W}_θ to transform the sample-specific class center embeddings to the sample-specific kernels as:

$$\mathbf{W}_\phi = \mathcal{H}_\theta(E, \mathbf{W}_\theta), \quad (3)$$

where \mathbf{W}_ϕ is the sample-specific kernels conditioned on the corresponding class center embeddings. We use group 1×1 convolution as the projection.

The generated filters are finally applied to each position of the input features F as:

$$Y = \mathcal{H}_\phi(F, \mathbf{W}_\phi) = \mathcal{H}_\phi(F, \mathcal{H}_\theta(\frac{P \times F^T}{N}, \mathbf{W}_\theta)), \quad (4)$$

where $\mathcal{H}_\phi(\cdot)$ indicates the convolution, while \times is the matrix multiplication, $N = H \times W$, H and W is the height and

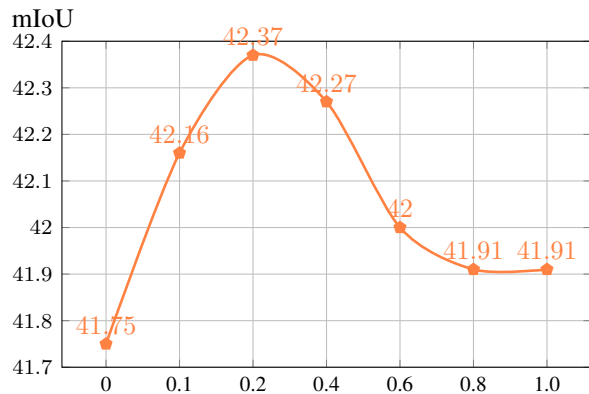


Fig. 3. **Influence of the loss weights for the Soft Dice Loss.** Different loss weights achieve similar results, indicating that the Soft Dice Loss is robust. Here, we choose $\lambda = 0.2$ as default.

width of the F. In other words, each generated weight/kernel correlates on the feature maps to highlight the pixels belong to the same category as the prediction map.

c) *Relation to other conditional architectures:* Different from normal networks, conditional architectures can achieve dynamic kernels. Dynamic filter networks [28] generates the convolution filters conditioned on the input. PAC convolution [29] dynamically modifies the kernel with an adapting kernel. CondINS [30] applies this design to the instance segmentation task, generating the parameters of the mask sub-network for each instance. SVCNet [31] learns a semantic correlation dependent shape-variant context. CondConv [32] and Dynamic Convolution [33] learn a series of weights to mix the corresponding convolution kernels for each sample, increasing the model capacity. Different from these methods, we employ the explicit supervision on the conditional generation process.

C. Overall Architecture

The proposed conditional classifier is flexible to be integrated into almost arbitrary FCN architectures. The architecture can replace the original classifier (the last layer of the architecture) with the proposed conditional classifier directly. The feature extractor outputs the embedding features, then the coarse probability maps are predicted. With the probability maps, we can aggregate class features as the sample-specific class center embeddings, then generate the sample-specific kernels to output the final predictions.

The overall loss function of the framework equipped with the conditional classifier can be formulated as:

$$L_{overall} = \lambda L_{prob} + L_{seg}, \quad (5)$$

where L_{prob} and L_{seg} denote the loss of the coarse probability maps and the loss of the conditional classifier, respectively. We set λ to 0.2 in this work to balance these two losses. We will give further comparisons to discuss the influence of λ at the experimental section. L_{seg} is the Cross Entropy Loss, while L_{prob} is the Soft Dice Loss [34] due to its effectiveness and

TABLE I
DIFFERENT LOSS FUNCTIONS FOR COARSE PROBABILITY MAPS

model, R50	mIoU(%)	picAcc(%)
FCN baseline	35.94	77.39
w/o supervision	41.75	79.89
w/ BCE Loss	40.43	79.67
w/ Soft Dice Loss	42.37	79.99

TABLE II
COMPARISON OF CONDITIONAL CLASSIFIER AND GLOBAL CLASSIFIER

classifier	FCN	PSPNet	DeeplabV3	DeeplabV3+
<i>global</i>	35.94	41.13	42.42	42.72
<i>conditional</i>	42.37	42.42	43.71	43.76
Δ	+6.43	+1.29	+1.29	+1.04

stability in training for class imbalance issue. The Soft Dice Loss is defined as:

$$L_{Dice} = 1 - \frac{2 \sum_i^N p_i q_i}{\sum_i^N p_i^2 + \sum_i^N q_i^2 + \epsilon}, \quad (6)$$

where $p_i \in \mathcal{R}^C$ is the probability vector of the probability maps, while $q_i \in \mathcal{R}^C$ is a one-hot encoding vector of the corresponding ground truth masks, $N = H \times W$, ϵ prevents division by zero.

III. EXPERIMENTS

We evaluate our approach on two scene segmentation datasets, i.e., ADE20K and PASCAL-Context. We perform a comprehensive ablation on ADE20K dataset, and report the comparisons with other methods on ADE20K and PASCAL-Context datasets.

A. Setting

a) *Datasets:* ADE20K [35] is a scene understanding dataset, containing 20K training images and 2K validation images. It has up to 150 category labels for challenging scenes.

PASCAL-Context [36] provides comprehensive scene understanding for both stuff and thing. It can be divided into 4,998 images for training and 5,105 images for testing. The most common 59 categories are used for evaluation.

b) *Training:* The network is trained on 8 NVIDIA V100 GPUs with mini-batch 16 per GPU. We adopt SGD optimizer with 0.9 momentum and the initial learning rate of $4e^{-3}$ for ADE20K, $1e^{-3}$ for PASCAL-Context. The ‘‘poly’’ learning rate [23], [24], [37] strategy is employed for the training process, in which the learning rate is multiplied by $(1 - \frac{iter}{max_iter})^{0.9}$. We use the synchronized batch normalization to train our networks. The total training iterations are 160K and 80K for ADE20K and PASCAL-Context datasets, respectively.

The input image size is cropped to 512×512 for ADE20K, and 480×480 for PASCAL-Context. Each image will go through a series of data augmentations, containing random flipping, random scale ([0.5, 2.0]) for both datasets.

TABLE III
EVALUATION ON THE ADE20K VALIDATION SET

model	reference	backbone	mIoU(%)	picAcc(%)
UperNet [38]	ECCV2018	ResNet-101	42.66	81.01
PSPNet [19]	CVPR2017	ResNet-269	44.94	81.69
PSANet [39]	ECCV2018	ResNet-101	43.77	81.51
EncNet [40]	CVPR2018	ResNet-101	44.65	81.69
CFNet [41]	CVPR2019	ResNet-101	44.89	–
ANL [42]	ICCV2019	ResNet-101	45.24	–
OCRNet [43]	ECCV2020	ResNet-101	45.28	–
APCNet [44]	CVPR2019	ResNet-101	45.38	–
RGNet [18]	ECCV2020	ResNet-101	45.80	81.76
CPNet [23]	CVPR2020	ResNet-101	46.27	81.38
DeeplabV3+ [37]	ECCV2018	ResNet-101	46.35	82.40
CondNet		ResNet-101	<u>47.38</u>	<u>82.49</u>
CondNet		ResNest-101	47.54	82.51

c) *Testing*: We adopt the sliding-window evaluation strategy. For the final results, following [19], [23], [37], we average the predictions of multiple scaled ([0.5, 1.75]) and flipped inputs to improve the performance further. In addition, we adopt the pixel accuracy (pixAcc) and mean IoU (mIoU) metrics for ADE20K, and mIoU for PASCAL-Context.

B. Ablation Study

We perform ablative evaluations on ADE20K validation set to demonstrate the effectiveness of our approach. We adopt the pre-trained ResNet-50 [13] as the backbone and the training iterations are 80K.

a) *Loss function*: Table I compares different loss functions for the coarse probability maps. We adopt the FCN based on ResNet-50 as our baseline. Without explicit supervision, the proposed classifier has achieved 5.81 mIoU increase. As shown, the Binary Cross Entropy (BCE) Loss achieves slightly worse results than the conditional classifier without supervision. It is because the majority of the pixels belong to the background for some certain category. The imbalance issue is hard for the BCE Loss. The Soft Dice Loss is designed to mitigate this issue. Therefore, this classifier with the Soft Dice Loss achieves 6.43 point gain. Figure 3 illustrates the influence of the loss weights λ . We choose $\lambda = 0.2$ as default.

b) *Conditional classifier vs. global classifier*: We apply the conditional classifier and global classifier to different approaches, including FCN, PSPNet, DeeplabV3, DeeplabV3+, respectively. The comparison of the dense recognition capability can be quantitatively measured by the performance contrast. Table II shows that the proposed conditional classifier achieves better performance than the global classifier. Specifically, the conditional classifier improves FCN by 6.43% mIoU, PSPNet by 1.29% mIoU, DeeplabV3 by 1.29% mIoU, and DeeplabV3+ by 1.04% mIoU, respectively. On the other hand, Table II also indicates that the conditional classifier is simple and flexible to integrate into the existing FCN architectures.

TABLE IV
EVALUATION ON THE PASCAL-CONTEXT VALIDATION SET

model	reference	backbone	mIoU(%)
PSPNet [19]	CVPR2017	ResNet-101	47.8
DeeplabV3+ [37]	ECCV2018	ResNet-101	48.3
CCL [46]	CVPR2018	ResNet-101	51.6
EncNet [40]	CVPR2018	ResNet-101	51.7
DANet [47]	CVPR2019	ResNet-101	52.6
SVCNet [31]	CVPR2019	ResNet-101	53.2
ANL [42]	ICCV2019	ResNet-101	52.8
CPNet [23]	CVPR2020	ResNet-101	53.9
RGNet [18]	ECCV2020	ResNet-101	53.9
CFNet [41]	CVPR2019	ResNet-101	54.0
APCNet [44]	CVPR2019	ResNet-101	54.7
OCRNet [43]	ECCV2020	ResNet-101	54.8
CondNet		ResNet-101	<u>56.0</u>
CondNet		ResNest-101	57.0

C. Results

We employ the proposed conditional classifier to DeeplabV3+ [37] (called **CondNet**) to compare with other methods on two datasets: ADE20K and PASCAL-Context.

a) *ADE20K*: The results of our method and other state-of-the-art methods are reported in Table III. Based on ResNet-101 [13], CondNet achieves 47.38% mIoU and 82.49% picAcc, significantly outperforming DeeplabV3+ by 1.03 points, CPNet by 1.11 points, RGNet by 1.58 points. With more powerful backbone networks, ResNest-101 [45], our CondNet achieves 47.54% mIoU. Besides, we train the CondNet on the train+val set and submit the results on test set. The CondNet based on ResNet-101 achieves a final score of 0.5742, while the CondNet based on ResNest-101 achieves 0.5754.

b) *PASCAL-Context*: Table IV reports the comparison results of our networks and other state-of-the-art methods. With ResNet-101, our method achieves 56.0% mIoU and outperforms OCRNet by 1.2 points, APCNet by 1.3 points, CFNet by 2.0 points. With ResNest-101, CondNet improves the mIoU to 57.0% further.

IV. CONCLUSION

In this letter, we propose a conditional classifier to replace the traditional global classifier (1×1 convolution for prediction) in the FCN architecture. For each input sample, this novel classifier aggregates the features of each category as the sample-specific class centers, and dynamically generates the corresponding kernels. The kernels attend on the intra-class distinction, leading to stronger recognition capability. The conditional classifier is easy and flexible to be integrated into almost arbitrary FCN architectures to improve the prediction results. Finally, the framework equipped this classifier (called CondNet) achieves new state-of-the-art results on two challenging datasets.

REFERENCES

- [1] Y. Huang, Z. Tang, D. Chen, K. Su, and C. Chen, "Batching soft iou for training semantic segmentation networks," *IEEE Signal Process. Lett.*, vol. 27, pp. 66–70, 2019. 1
- [2] J. Li, S. He, H.-C. Wong, and S.-L. Lo, "Proposal-driven segmentation for videos," *IEEE Signal Process. Lett.*, vol. 26, no. 8, pp. 1098–1102, 2019. 1
- [3] A. Arnab, S. Zheng, S. Jayasumana, B. Romera-Paredes, M. Larsson, A. Kirillov, B. Savchynskyy, C. Rother, F. Kahl, and P. H. Torr, "Conditional random fields meet deep neural networks for semantic segmentation: Combining probabilistic graphical models with deep learning for structured prediction," *IEEE Signal Process. Mag.*, vol. 35, no. 1, pp. 37–52, 2018. 1
- [4] Q. Zhou, W. Yang, G. Gao, W. Ou, H. Lu, J. Chen, and L. J. Latecki, "Multi-scale deep context convolutional neural networks for semantic segmentation," *World Wide Web*, vol. 22, no. 2, pp. 555–570, 2019. 1
- [5] L. Wang, D. Li, Y. Zhu, L. Tian, and Y. Shan, "Dual super-resolution learning for semantic segmentation," in *Proc. IEEE Conf. Comput. Vis. Pattern Recognit.*, 2020, pp. 3774–3783. 1
- [6] V. Badrinarayanan, A. Kendall, and R. Cipolla, "SegNet: A deep convolutional encoder-decoder architecture for image segmentation," *IEEE Trans. Pattern Anal. Mach. Intell.*, vol. 39, no. 12, pp. 2481–2495, 2017. 1
- [7] A. Geiger, P. Lenz, and R. Urtasun, "Are we ready for autonomous driving? the kitti vision benchmark suite," in *Proc. IEEE Conf. Comput. Vis. Pattern Recognit.*, 2012, pp. 3354–3361. 1
- [8] M. Cordts, M. Omran, S. Ramos, T. Rehfeld, M. Enzweiler, R. Benenson, U. Franke, S. Roth, and B. Schiele, "The cityscapes dataset for semantic urban scene understanding," in *Proc. IEEE Conf. Comput. Vis. Pattern Recognit.*, 2016. 1
- [9] Q. Zhou, Y. Wang, Y. Fan, X. Wu, S. Zhang, B. Kang, and L. J. Latecki, "AglNet: Towards real-time semantic segmentation of self-driving images via attention-guided lightweight network," *Applied Soft Computing*, vol. 96, p. 106682, 2020. 1
- [10] X. Liang, K. Gong, X. Shen, and L. Lin, "Look into person: Joint body parsing & pose estimation network and a new benchmark," *IEEE Trans. Pattern Anal. Mach. Intell.*, vol. 41, no. 4, pp. 871–885, 2018. 1
- [11] A. Krizhevsky, I. Sutskever, and G. E. Hinton, "Imagenet classification with deep convolutional neural networks," in *Proc. Adv. Neural Inf. Process. Syst.*, 2012. 1
- [12] K. Simonyan and A. Zisserman, "Very deep convolutional networks for large-scale image recognition," *Proc. Int. Conf. on Learn. Represent.*, 2015. 1
- [13] K. He, X. Zhang, S. Ren, and J. Sun, "Deep residual learning for image recognition," in *Proc. IEEE Conf. Comput. Vis. Pattern Recognit.*, 2016. 1, 4
- [14] G. Huang, Z. Liu, L. van der Maaten, and K. Q. Weinberger, "Densely connected convolutional networks," *Proc. IEEE Conf. Comput. Vis. Pattern Recognit.*, pp. 2261–2269, 2017. 1
- [15] J. Long, E. Shelhamer, and T. Darrell, "Fully convolutional networks for semantic segmentation," in *Proc. IEEE Conf. Comput. Vis. Pattern Recognit.*, 2015. 1
- [16] L.-C. Chen, G. Papandreou, I. Kokkinos, K. Murphy, and A. L. Yuille, "Semantic image segmentation with deep convolutional nets and fully connected crfs," *Proc. Int. Conf. on Learn. Represent.*, 2015. 1
- [17] J. Dai, H. Qi, Y. Xiong, Y. Li, G. Zhang, H. Hu, and Y. Wei, "Deformable convolutional networks," in *Proc. IEEE Int. Conf. Comput. Vis.*, 2017, pp. 764–773. 1
- [18] C. Yu, Y. Liu, C. Gao, C. Shen, and N. Sang, "Representative graph neural network," in *Proc. Eur. Conf. on Comput. Vis.* Springer, 2020, pp. 379–396. 1, 4
- [19] H. Zhao, J. Shi, X. Qi, X. Wang, and J. Jia, "Pyramid scene parsing network," *Proc. IEEE Conf. Comput. Vis. Pattern Recognit.*, 2017. 1, 4
- [20] L.-C. Chen, G. Papandreou, F. Schroff, and H. Adam, "Rethinking atrous convolution for semantic image segmentation," *arXiv*, 2017. 1
- [21] J. Fu, J. Liu, J. Jiang, Y. Li, Y. Bao, and H. Lu, "Scene segmentation with dual relation-aware attention network," *IEEE Trans. Neural Netw. Learn. Syst.*, pp. 1–14, 2020. 1
- [22] X. Wang, R. Girshick, A. Gupta, and K. He, "Non-local neural networks," *Proc. IEEE Conf. Comput. Vis. Pattern Recognit.*, 2018. 1
- [23] C. Yu, J. Wang, C. Gao, G. Yu, C. Shen, and N. Sang, "Context prior for scene segmentation," in *Proc. IEEE Conf. Comput. Vis. Pattern Recognit.*, 2020, pp. 12416–12425. 1, 3, 4
- [24] C. Yu, J. Wang, C. Peng, C. Gao, G. Yu, and N. Sang, "Learning a discriminative feature network for semantic segmentation," in *Proc. IEEE Conf. Comput. Vis. Pattern Recognit.*, 2018. 1, 3
- [25] J. Hu, L. Shen, and G. Sun, "Squeeze-and-excitation networks," *Proc. IEEE Conf. Comput. Vis. Pattern Recognit.*, 2018. 1
- [26] C. Yu, J. Wang, C. Peng, C. Gao, G. Yu, and N. Sang, "Bisenet: Bilateral segmentation network for real-time semantic segmentation," in *Proc. Eur. Conf. on Comput. Vis.*, 2018, pp. 325–341. 1
- [27] C. Yu, C. Gao, J. Wang, G. Yu, C. Shen, and N. Sang, "Bisenet v2: Bilateral network with guided aggregation for real-time semantic segmentation," *arXiv*, 2020. 1
- [28] X. Jia, B. De Brabandere, T. Tuytelaars, and L. V. Gool, "Dynamic filter networks," in *Proc. Adv. Neural Inf. Process. Syst.*, 2016, pp. 667–675. 3
- [29] H. Su, V. Jampani, D. Sun, O. Gallo, E. Learned-Miller, and J. Kautz, "Pixel-adaptive convolutional neural networks," in *Proc. IEEE Conf. Comput. Vis. Pattern Recognit.*, 2019, pp. 11166–11175. 3
- [30] Z. Tian, C. Shen, and H. Chen, "Conditional convolutions for instance segmentation," in *Proc. Eur. Conf. on Comput. Vis.*, 2020. 3
- [31] H. Ding, X. Jiang, B. Shuai, A. Q. Liu, and G. Wang, "Semantic correlation promoted shape-variant context for segmentation," in *Proc. IEEE Conf. Comput. Vis. Pattern Recognit.*, 2019, pp. 8885–8894. 3, 4
- [32] B. Yang, G. Bender, Q. V. Le, and J. Ngiam, "Condconv: Conditionally parameterized convolutions for efficient inference," in *Proc. Adv. Neural Inf. Process. Syst.*, 2019, pp. 1307–1318. 3
- [33] Y. Chen, X. Dai, M. Liu, D. Chen, L. Yuan, and Z. Liu, "Dynamic convolution: Attention over convolution kernels," in *Proc. IEEE Conf. Comput. Vis. Pattern Recognit.*, 2020, pp. 11030–11039. 3
- [34] F. Milletari, N. Navab, and S.-A. Ahmadi, "V-net: Fully convolutional neural networks for volumetric medical image segmentation," in *Int. Conf. on 3D Vis.* IEEE, 2016, pp. 565–571. 3
- [35] B. Zhou, H. Zhao, X. Puig, S. Fidler, A. Barriuso, and A. Torralba, "Semantic understanding of scenes through the ade20k dataset," *Int. J. Comput. Vis.*, vol. 127, pp. 302–321, 2018. 3
- [36] R. Mottaghi, X. Chen, X. Liu, N.-G. Cho, S.-W. Lee, S. Fidler, R. Urtasun, and A. Yuille, "The role of context for object detection and semantic segmentation in the wild," in *Proc. IEEE Conf. Comput. Vis. Pattern Recognit.*, 2014. 3
- [37] L.-C. Chen, Y. Zhu, G. Papandreou, F. Schroff, and H. Adam, "Encoder-decoder with atrous separable convolution for semantic image segmentation," in *Proc. Eur. Conf. on Comput. Vis.*, 2018, pp. 801–818. 3, 4
- [38] T. Xiao, Y. Liu, B. Zhou, Y. Jiang, and J. Sun, "Unified perceptual parsing for scene understanding," in *Proc. Eur. Conf. on Comput. Vis.*, 2018, pp. 418–434. 4
- [39] H. Zhao, Y. Zhang, S. Liu, J. Shi, C. C. Loy, D. Lin, and J. Jia, "PSANet: Point-wise spatial attention network for scene parsing," in *Proc. Eur. Conf. on Comput. Vis.*, 2018. 4
- [40] H. Zhang, K. Dana, J. Shi, Z. Zhang, X. Wang, A. Tyagi, and A. Agrawal, "Context encoding for semantic segmentation," in *Proc. IEEE Conf. Comput. Vis. Pattern Recognit.*, 2018, pp. 7151–7160. 4
- [41] H. Zhang, H. Zhang, C. Wang, and J. Xie, "Co-occurrent features in semantic segmentation," in *Proc. IEEE Conf. Comput. Vis. Pattern Recognit.*, 2019, pp. 548–557. 4
- [42] Z. Zhu, M. Xu, S. Bai, T. Huang, and X. Bai, "Asymmetric non-local neural networks for semantic segmentation," in *Proc. IEEE Int. Conf. Comput. Vis.*, 2019, pp. 593–602. 4
- [43] Y. Yuan, X. Chen, and J. Wang, "Object-contextual representations for semantic segmentation," in *Proc. Eur. Conf. on Comput. Vis.*, 2020. 4
- [44] J. He, Z. Deng, L. Zhou, Y. Wang, and Y. Qiao, "Adaptive pyramid context network for semantic segmentation," in *Proc. IEEE Conf. Comput. Vis. Pattern Recognit.*, 2019, pp. 7519–7528. 4
- [45] H. Zhang, C. Wu, Z. Zhang, Y. Zhu, Z. Zhang, H. Lin, Y. Sun, T. He, J. Mueller, R. Manmatha *et al.*, "Resnest: Split-attention networks," *arXiv preprint arXiv:2004.08955*, 2020. 4
- [46] H. Ding, X. Jiang, B. Shuai, A. Qun Liu, and G. Wang, "Context contrasted feature and gated multi-scale aggregation for scene segmentation," in *Proc. IEEE Conf. Comput. Vis. Pattern Recognit.*, 2018, pp. 2393–2402. 4
- [47] J. Fu, J. Liu, H. Tian, Z. Fang, and H. Lu, "Dual attention network for scene segmentation," *Proc. IEEE Conf. Comput. Vis. Pattern Recognit.*, 2019. 4